UAV Path Planning for Maximum-Information Sensing in Spatiotemporal Data Acquisition

By:
Andreas Nordby Vibeto
andreanv@stud.ntnu.no

Supervisor: **Tor Arne Johansen**

Co-supervisor: João F. Fortuna

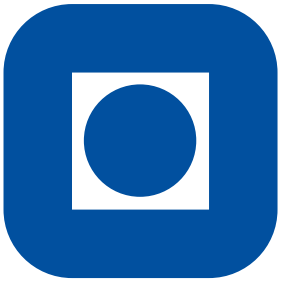

NTNU

February, 2017

Contents

Chapter 1

Introduction

Unmanned Aerial Vehcles (UAV) are today widely used in ground observation, and by equipping them with different sensors they can be used in different situations. While the use of UAV eases many cases of ground obsercation, there are some difficulties related to the attitude of the aircraft. When the sensor is attached directly to the aircraft the sensor will be coupled with the UAVs states, so that any change in the UAV states will cause a change in what is actually observed by the sensor.

A common solution to decouple the sensor from the UAV states is to attach the sensor to a gimbal which will countaract most of the movements of the UAV. While this is a good solution for decoupling, it raises some new issues regarding its weight and size. As one of the benefits of UAVs is their small size the gimbal can quickly be too big and heavy for the UAV, and it may give less effective aerodynamics. This may again lead to increased fuel consumption for the UAV.

This paper will investigate methods to reduce image errors caused by the UAVs attitude, while also avoiding the extra costs associated with a gimbal. This will be accomplished by optimizing a pre-defined curved path that is to be observed with a model of the UAV. The control method will be developed with a hyperspectral pushbroom camera that is fixed to the UAV in mind.

1.1 Optimization

Optimization techniques is a common way to control UAVs, both as online and offline systems. An nonline optimization system can measure the current states of the aircraft, and based on that calculate the optimal input depending on the final state. An offline system, which will be developed in this paper, calculates the states and inputs before the flight has actually taken place. An offline solution is often simpler as an optimization system tends to require a great deal of computing power.

1.2 Hyperspectral Imaging

The control method developed in this paper will be developed with the use of a fixed hyperspectral, pushbroom sensor in mind. A hyperspectral sensor/camera makes it possible to accurately detect types of material from the UAV by sensing the wavelength of the received light.

1.2.1 Description

Hyperspectral imaging uses basics from spectroscopy to create images, which means that the basis for the images is the emitted or reflected light from materials [1]. The amount of light that is reflected by a material at different wavelengths is determined by several factors, and this makes it possible to distinguish different materials from each other. The reflected light is passed through a grate or a prism that splits the light into different wavelength bands, so that it can be measured by a spectrometer.

When using a hyperspectral camera for ground observation from a UAV, it is very likely that one pixel of the camera covers more than one type of material on the ground. This means that the observed wavelengths will be influenced by more than one type of material. This is called a composite or mixed spectrum [1], and the spectra of the different materials are combined additively. The combined spectra can be split into the different spectra that it is build up of by noise removal and other statistical methods which will not be covered here.

1.2.2 UAV Ground Observation

Hyperspectral imaging is already being used for ground observation from UAVs. Its ability to distinguish materials based on spectral properties means that it can be used to retrieve information that normal cameras are not able to. For example in agriculture it can be used to map damage to trees caused by bark beetles [2], or it can be used to measure environmental properties, for example chlorophyl fluorescense, on leaf-level in a citrus orchard [3].

Systems for ground observation with hyperspectral cameras can be very complex, which often leads to heavy systems. In [4], a lightweight hyperspectral mapping system was created for the use with octocopters. The purpose of the system is to map agricultural areas using a spectrometer and a photogrammetric camera, and the final ”ready-to-fly” weight of the system is 2.0 kg. The resolution of the final images made it possible to gather information on a single-plant basis, and the georeferencing accuracy was off by only a few pixels.

The tests were performed at a low altitude, maximum 120 m. While this was mainly because of local regulations, it also gave a benefit as there was less atmosphere disturbance in the measurements. The UAVs orientation data combined with surface models was used when recovering the positional data in the images. However, they found

that externally produced surface models was not accurate enough as they do not take vegetation into consideration. For this reason they supplemented the existing surface models with information gathered during flight.

Chapter 2

Theory

2.1 Kinematics

When the camera is fixed to the aircraft body, what is actually captured by the camera, the camera footprint, depends on the angles of the aircraft. The equations needed to express the position of the centre and outer points of the camera footprint will be given here. The kinematic model for the UAV used in this paper will also be given here.

2.1.1 UAV States

The position of the UAV will be given using the North East Down (NED) coordinate frame, denoted $\{n\}$:

$$\mathbf{p}_{b/n}^{n} = \begin{bmatrix} N \\ E \\ D \end{bmatrix} = \begin{bmatrix} x_n \\ y_n \\ z_n \end{bmatrix}. \tag{2.1.1}$$

The attitude of the UAV will be given as Euler-angles:

$$\mathbf{\Theta}_{nb} = \begin{bmatrix} \phi \\ \theta \\ \psi \end{bmatrix} \tag{2.1.2}$$

with corresponding angular velocities:

$$\dot{\mathbf{\Theta}}_{nb} = \begin{bmatrix} p \\ q \\ r \end{bmatrix}. \tag{2.1.3}$$

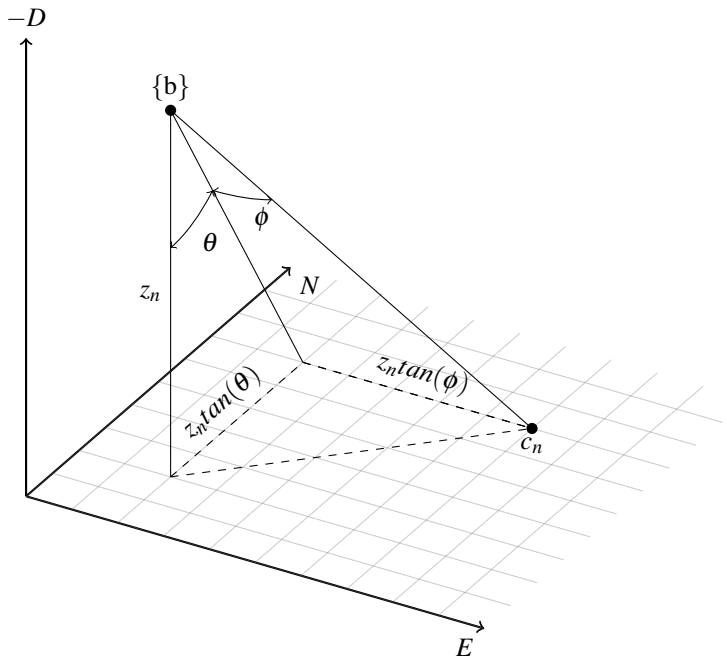

Figure 2.1: Illustration of how the aircraft attitude influence the camera position.

ADD WIND KINEMATICS

2.1.2 Camera Footprint

The camera footprint is coupled with all of the three angles given in $\boldsymbol{\Theta}$. The position of the camera footprint will be calculated using forward kinematics, and the "SITUATION" is shown in figure 2.1.

Centre Position

The attitude of the UAV is given in the body frame $\{b\}$ and the height z_n is given in the NED frame $\{n\}$, and the model assumes flat earth. The position of the footprint centre point $\mathbf{c}_b^b$ in the body frame $\{b\}$ is expressed as the geometric (???) distance from the UAV position to the footprint centre point:

$$\mathbf{c}_b^b = \begin{bmatrix} c_{x/b}^b \\ c_{y/b}^b \end{bmatrix} = \begin{bmatrix} z_n tan(\theta) \\ z_n tan(\phi) \end{bmatrix}. \tag{2.1.4}$$

The coordinates of the camera position in $\{n\}$ can be found by rotating the point $\mathbf{c}_b^b$ with respect to the aircraft heading ψ, and by translating the rotated point to the aircrafts position in the $\{n\}$ frame. The rotation matrix for rotating with respect to the heading is given as

$$\mathbf{R}_{z,\psi} = \begin{bmatrix} cos(\psi) & -sin(\psi) \\ sin(\psi) & cos(\psi) \end{bmatrix}. \tag{2.1.5}$$

The final expression for the camera footprint centre position $\mathbf{c}^n$ in the $\{n\}$ frame then becomes:

$$\begin{aligned} \mathbf{c}^n &= \mathbf{p} + \mathbf{R}_{z,\psi}\mathbf{c}_b^b \\ &= \begin{bmatrix} x_n \\ y_n \end{bmatrix} + \mathbf{R}_{z,\psi} \begin{bmatrix} x_{x/b}^b \\ c_{y/b}^b \end{bmatrix} \end{aligned} \tag{2.1.6}$$

Edge Points

A hyperspectral pushbroom sensor captures images in a line, and the centre point of the camera footprint does not express the entire area that is captured by the sensor. The edge points of the camera footprint are calculated with respect to the sensor's field of view, as shown in figure 2.2. These points $\mathbf{e}$ can be found by altering 2.1.4:

$$\mathbf{e}_{1,b}^b = \begin{bmatrix} z_n tan(\theta) \\ z_n tan(\phi + \sigma) \end{bmatrix}, \ \mathbf{e}_{2,b}^b = \begin{bmatrix} z_n tan(\theta) \\ z_n tan(\phi - \sigma) \end{bmatrix} \tag{2.1.7}$$

The steps for writing the edge points $\mathbf{e}$ in the $\{n\}$ is similar as in equation 2.1.6:

$$\mathbf{e}^n = \mathbf{p} + \mathbf{R}_{z,\psi}\mathbf{e}_b^b \tag{2.1.8}$$

2.2 Optimization

2.2.1 MPC Method

2.2.2 Problem Definition

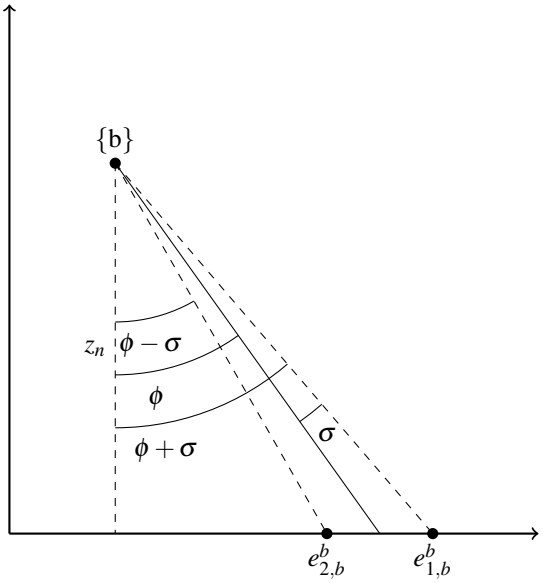

Figure 2.2: Illustration of how the field of view for a pushbroom sensor is calculated.

Bibliography

[1] Randall B. Smith. *Introduction to Hyperspectral Imaging*. MicroImages, Inc., 2012.

[2] R. Näsi, E. Honkavaara, P. Lyytikäinen-Saarenmaa, M. Blomqvist, P. Litkey, T. Hakala, N. Viljanen, T. Kantola, T. Tanhuanpää, and M. Holopainen. Using uav-based photogrammetry and hyperspectral imaging for mapping bark beetle damage at tree-level. *Remote Sensing*, 7(15467-15493), 2015.

[3] P. J. Zarco-Tejada, V. González-Dugo, and J. A. J. Berni. Fluorescence, temperature and narrow-band indices acquired from a uav platform for water stress detection using a micro-hyperspectral imager and a thermal camera. *Remote Sensing of Environment*, 117(322-337), 2012.

[4] J. Suomalainen, N. Anders, S. Iqbal, G. Roerink, J. Franke, P. Wenting, D. Hünniger, H. Bartholomeus, R. Becker, and L. Kooistra. A lightweight hyperspectral mapping system and photogrammetric processing chain for unmanned aerial vehicles. *Remote Sensing*, 6(11013-11030), 2014.